IOSR Journal of Electrical and Electronics Engineering (IOSR-JEEE)
e-ISSN: 2278-1676, p-ISSN: 2320-3331, Volume 18, Issue 3 Ser. I (May. – June. 2023), PP 01-23
www.iosrjournals.org

Lightning Search Algorithm For Mitigation Of Power Quality Using UPQC Controller: A Comparative Approach

Ms Geena.S,
Research Scholar,Dept of Electrical and Electronics Engineering,College of Engineering,Trivandrum
Dr.J S Savier ,
Former Head, Dept of Electrical and Electronics Engineering,College of Engineering,Trivandrum

Abstract:
Hybrid Renewable Energy Resource System (HRES) is made up of PV, Wind and Battery. PV and Wind inputs are irradiance and Wind in which energy is generated. The battery is used as an energy storage unit to store most of the energy produced and can be used to meet the need for load under critical and environmental conditions. Unified Power Quality Controller to reduce power quality related issues such as sag, swell, harmonics etc. in the HRES system connected mainly owing to the non-linear load condition. So this paper proposes a Lightning Search Algorithm (LSA) with Unified Power Quality controller (UPQC) to solve PQ problems in the HRES system. The results obtained specify that the proposed LSA algorithm has several advantages in various aspects such as early convergence and obtaining optimized fitness value compared to other algorithms such as Harris Hawks Optimizer (HHO), Gray Wolf Optimization (GWO) and Modified Particle Swarm Optimization (PSO).Therefore the proposed system is used on the MATLAB / Simulink platform to ensure performance at voltage sag, current sag, real power, active power and in terms of complete harmonic distortion (THD's).

Keywords: *PV (Photovoltaic), Wind, battery, Power Quality (PQ), UPQC (Unified Power Quality Controller), Lightning Search Algorithm(LSA) Harris Hawks Optimizer (HHO), Grey Wolf Optimization (GWO), Modified Particle Swarm Optimization (PSO), THD (Total Harmonic Distortion).*

Date of Submission: 19-04-2023 Date of Acceptance: 02-05-2023

I. Introduction

RES (Renewable Energy Sources) has played a key role in power generation over the past decades. The base of the hybrid power system is lying on the WECS (Wind Energy Conversion System) and the Photovoltaic (PV) system. The system does not provide the required reactive power during system defects. Hence, the voltage profile at the common connection point is on fluctuate and negative effects have been observed on these streams (Mohammed I. Mosaad, 2020). In addition to these voltages, the system stability, the power factor and the PQ, including the performance of the power system loading, if not properly controlled, can spread to undesirable surfaces based on some grid code. These grids Preparations for fault ride through (FRT) were made for continuous operation and determination of faults and trip zones (Thumu, Raghu, 2020; A. Ghosh, 2002).

The fact device has many merits and delivery as high speed and flexibility. For the system development the different sources are connected in common point. For this reason the system is more efficient and flexible (Dutta, 2015; Sarker, 2014). The Harmonics developed different sources connected to the grid were removed by using the UPQC. Collaborative power is the best tool of the truth that families study in this book (Vandana chaudhary, 2019).

Between the current transfer systems, the UPQC can control the power system (Chong, 2009). In the context of changing the current online system, new opportunities are being created for power control as well as to drive online growth (Ghadimi, 2013; Lashkar Ara, 2011). Best wolf algorithm (E. Babaei et al., 2011), Gray wolf algorithm (Ranjan Kumar Mallick et al., 2016), Whale Optimization algorithm (K. Aravindhan et al, 2019), Harris Hawks algorithm (Mohammad Zohrul Islamet al., 2019) and data analytics (Serhat Duman, 2019) are different methods of algorithms to overcome the problem of power

The power control system of photovoltaic-wind hybrid power is provided by UPQC using intelligent control system. This paper organized as follows: Section2 deals with the block diagram of the proposed system. Unified Power Flow controller is presented in section3 and section4 design an overview of optimization

technique details are given. Simulation results are given in section 5 and section6 concludes this research work.

II. The proposed system Block Diagram description

The HRES system required is a combination of PV and WT applied online. BESS is designed to meet the burden under extreme environmental conditions since these sources are volatile. Due to unplanned load and sudden load, PQ problems are created in the HRES system. Due to this voltage weak and reactive power mismatches are created. In this paper, PQ problems such as voltage sag, sag current and THD are solved. To overcome such problems, HRES system uses UPQC to improve the voltage system. Operating system optimization is used as an LSA. This diagram is a series of diagrams as shown in Fig.1, which consists of a diffuser and a PV-Wind coil connected to an inverter to rotate through a DC-link capacitor.

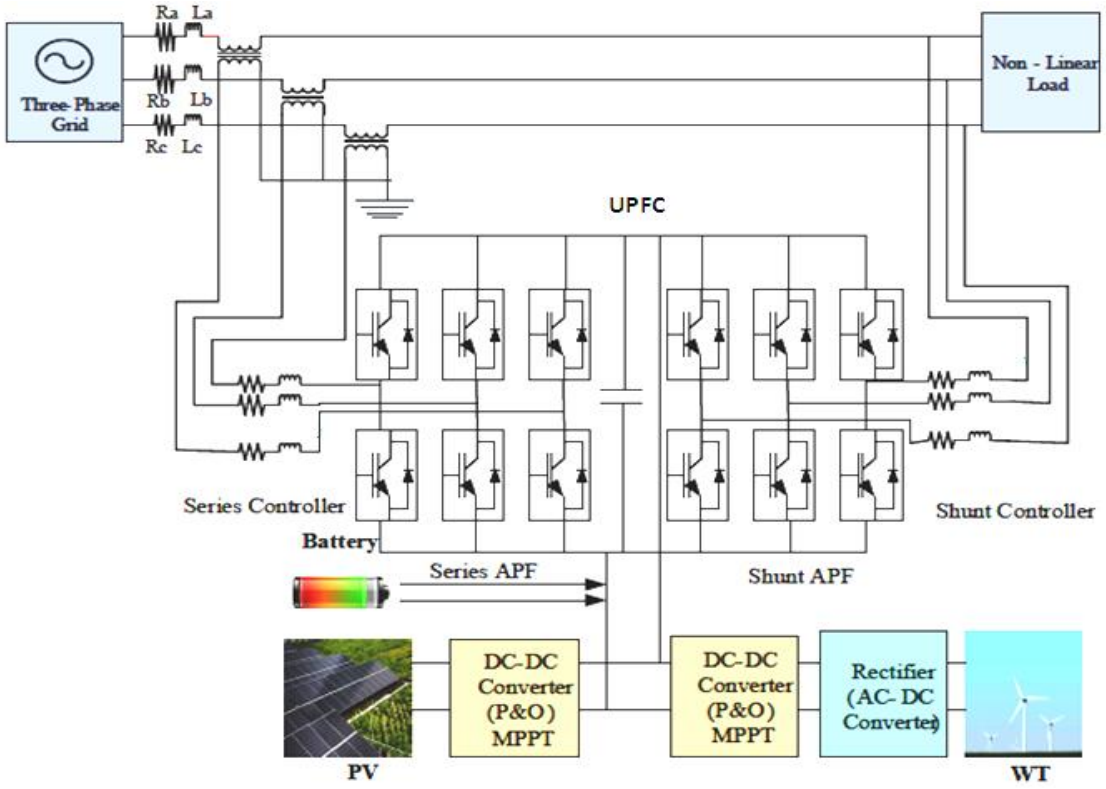

Figure1: Block diagram of grid-connected HRES

BESS (Battery Storage System) is designed for saving power and supply during system failure. Through the implementation and testing of (P&O) MPPT, PV and atmospheric energy are extracted. From the LSA a reference is made to the DC connection. The DC connection voltage is applied for its default during the absence of solar power. The strength of HRES is considered to be mainly due to fault, non-linear load, and accidental load in the grid area.

To overcome all the problems and hard work, this system was developed at UPQC which compensates the problem by system control using shunt and shunt controllers. Payment can be made during the sag mode by providing a good value for the PI manager who cleans and activates the required capacity by selecting the best value score on the PI manager. PI management is performed in an LSA designed to select the values required to perform management functions during PQ mode.

In general, the required device is a combination of the shunt and the power filtration system as shown in Fig. 2.

Using the current reference, the current error is calculated which will be compensated by the PI based LSA

controller that delivers SAPF requirements.

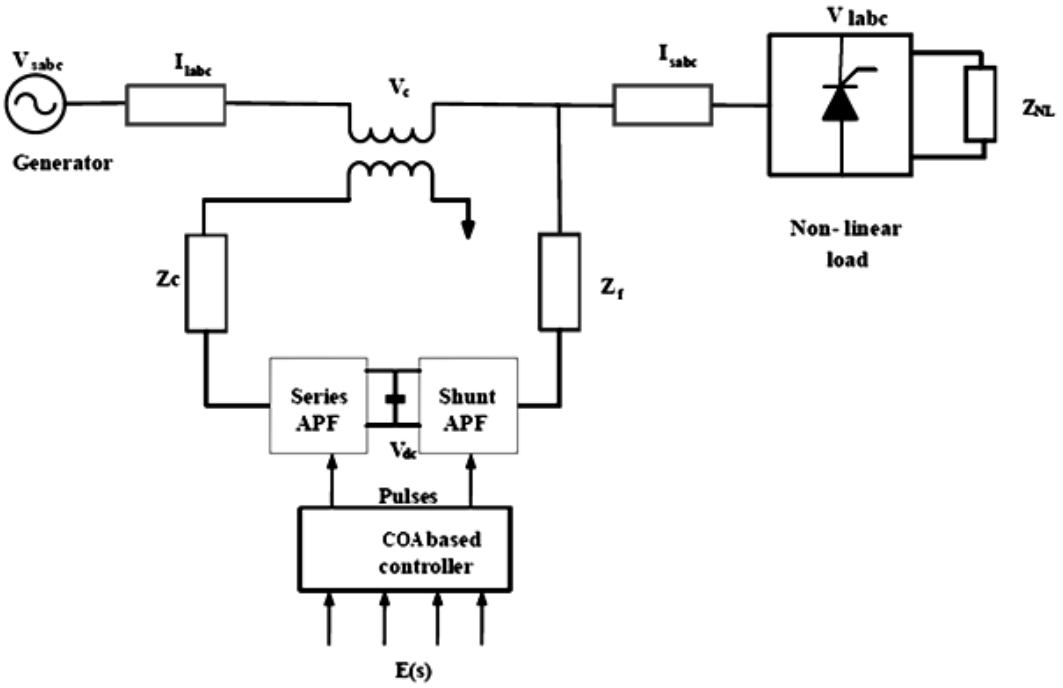

Fig. 2 Architecture of UPQC

To improve the operating system as well as to obtain two or more energy dissipation energy that is integrated into the hybrid system. The power supply components are PV, Wind and Battery are considered.

Photovoltaic

The photo-voltaic system of the sun works on a principle when the electric field fall on a solar cell. It converts solar energy into electrical energy. The photovoltaic system has one major component, namely photovoltaic cells that generate energy. However, other devices to control, modify and conserve power are also needed, for example. PV module, battery, controller and inverter. Batteries are used to store electricity and for use without sunlight. The photovoltaic system and its components are described in detail in the block diagram shown in Figure.3

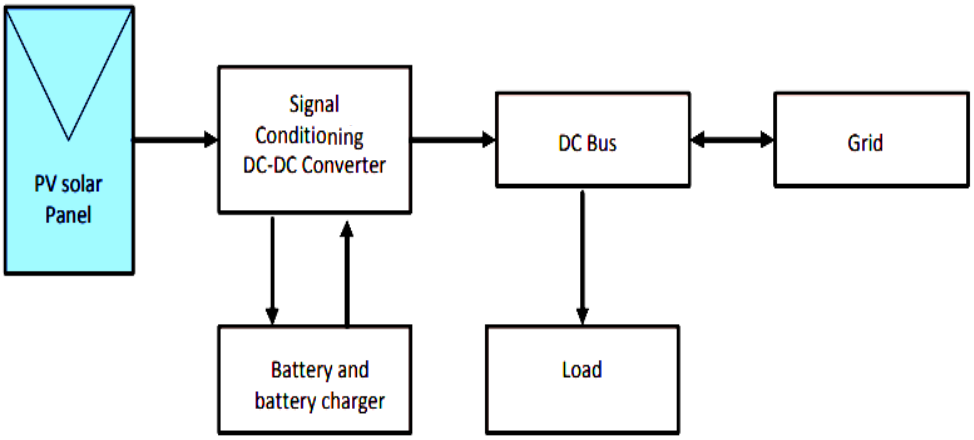

Figure 3: General block diagram of a photovoltaic system

By the modernization diode connected in parallel and the current supply a solar cell can be reflected. It takes its own structure and similar stability replaces similar systems and connections. Rs is the series resistance

which is due to interference with the direction of movement of electrons from 'n' to 'p' stop and similar stability is for the current stop. The circuit diagram of the PV cell is shown in Figure 4.

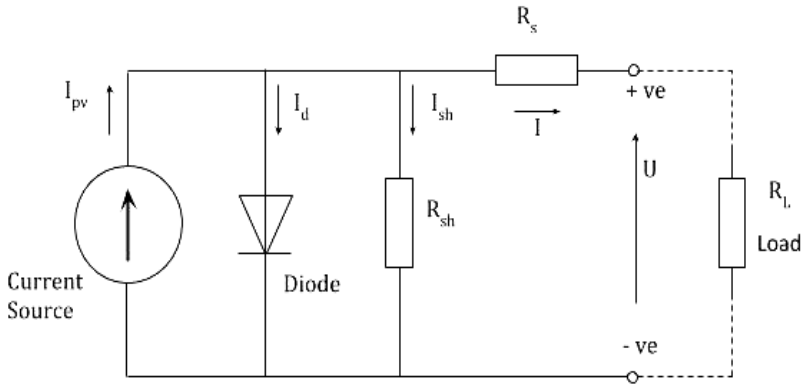

Figure 4 Equivalent circuit of a solar cell

The current output from the PV system is

$$I = I_{sc} - I_d \quad (1)$$

$$I_d = I_O(e^{\frac{qV_d}{KT}} - 1) \quad (2)$$

Where diode opposite saturation current is denoted as I_o , the charge of electron is denoted as q, the diode volatge is denoted asV_d, Boltzmann constant is denoted as k which is (1.38 * 10^(-19) J/K) and the junction temperature is denoted as T in Kelvin (K).

From equation 1 and equation 2

$$I = I_{sc} - I_o(e^{\frac{qV_d}{KT}} - 1) \quad (3)$$

By proper estimates,

$$I = I_{sc} - I_o(e^{q(\frac{V+IRs}{nKT})} - 1) \quad (4)$$

where, PV cell current is denoted as I, PV cell voltage is denoted as V and the diode ideality factor is denoted as n.

Wind Turbine

The Figure shown in Figure 5 is an example of the block diagram of the wind turbine (WT) system. The KE (kinetic energy) of the wind became to rotational motion and by using the gearbox it was the combustion chamber of the obtain and the generator. The generator function is to change the mechanical power into the electrical power. The AC voltage-DC converter is used in batteries connected in such a way that it can charge both the bidirectional converter circuit and the battery is charged [Tafticht, 2006].

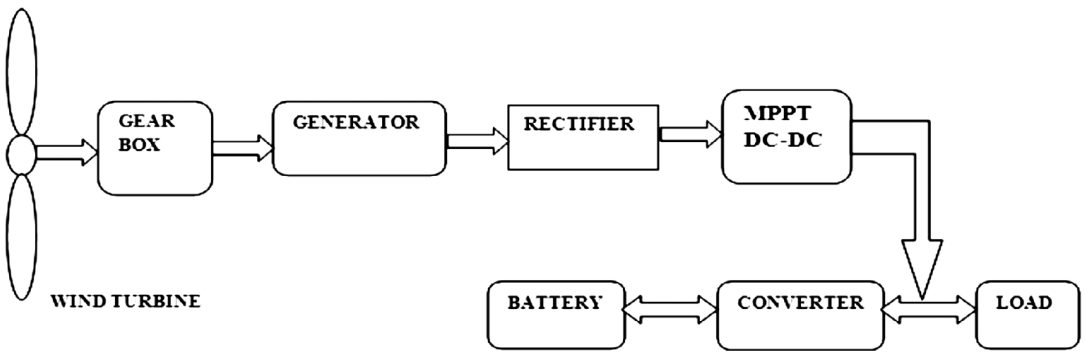

Figure 5 Wind energy system block diagram.

Figure 6 represents the circuit diagram of the wireless network. Wind turbines operate by converting the wind power at start-up into a constant electric current in the turbine of the electric field. The wind speed that will be available for the turntable depends on the wind speed and the angle of the turbine:

$$P_W = \frac{1}{2}\rho A V^3 \qquad (5)$$

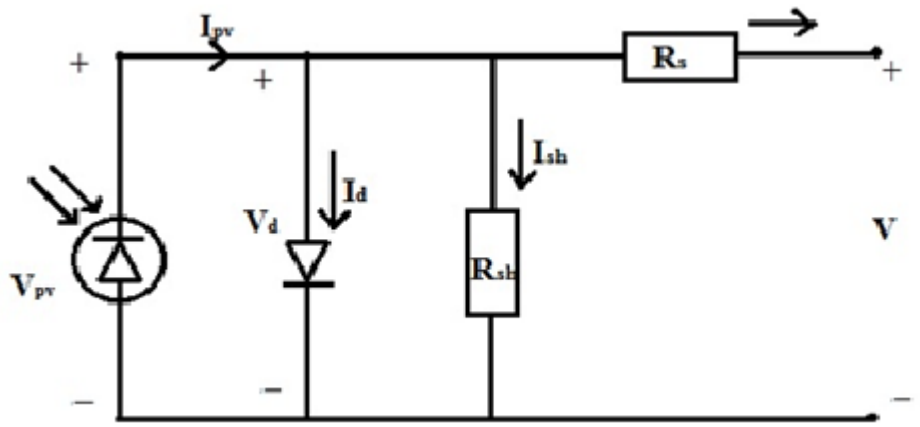

Figure 6 Equivalent circuit diagram of wind turbine

Where ρ is air thickness (Kg/m^3), A is swept part (m_2) and V is wind velocity (m/s). The most effective theoretic of any configuration of window air is 0.59. 59% of the electricity cannot be transferred with the help of wind by air conditioning. Air conditioners do not work at this maximum. The power of the cp coil on the input (1) and the removal of energy from the wind is thought of by:

$$P = \frac{1}{2}C_P\rho A V^3 \qquad (6)$$

The Cp rate is precisely for each turbine type then the characteristics of the wind speed at which the turbine is working. If we remember the other things in a whole wind turbine gadget only 10-30% of the power of the wind is simply changed to energy efficiency. Numerical power, defined as the energy dissipated from the rotor and the energy gained in the wind is:

$$C_P = \frac{P}{\frac{1}{2}\rho A V^3} = \frac{Power\ Extracted\ by\ Rotor}{Power\ Available\ in\ the\ wind} \qquad (7)$$

MPPT (Maximum Power Point Tracking)

Depending on the light, thermal energy and PV (electrical power and current strength) are provided by the sun. Tracing the point of efficient use of energy is made important consideration in the model of active solar systems. Under extreme weather conditions the P&O process is adopted to properly track the high power point (MPP).

Perturbation and Observation method

In this way, power conversion is considered as an MPPT agent. Here, in the increase in power, the next violence at work will be in the same place to get the MPP and with the decline, the effective disruption will be on the other side. The high power tracker works by periodically increasing or decreasing the power of the solar array. If a given disturbance leads to an increase (decrease) of the same force, the following disturbance is performed in the same (opposite) direction As it is a direct control method, the function is used directly without using a PI control [Femia, N, 2005].

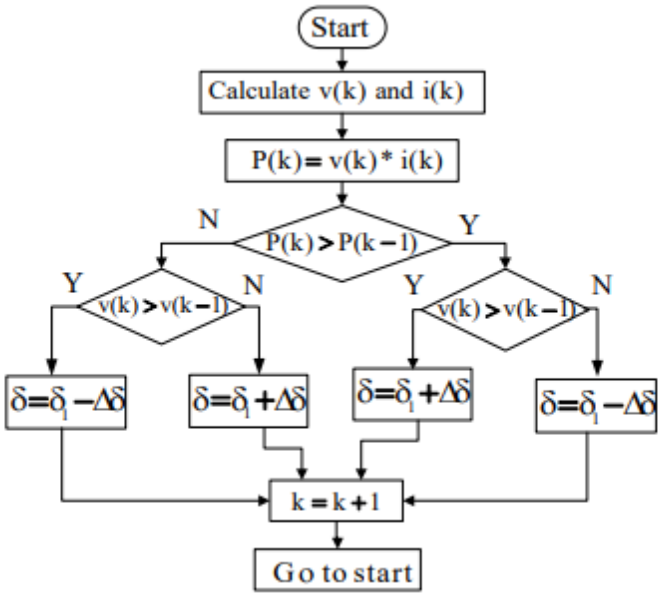

Fig. 7: Perturb and observe algorithm

The MPPT using the P and O algorithm corrects the power output from the PV range in small quantities and measures the power, when further power increases appear other changes are made in that direction until no increase in power is observed. The method described above is known as the perturb and observation method. Perturb & observation method can lead to high efficiency. **Perturb and observe algorithm** flowchart is shown in Figure. 7.

Battery

The batteries have a medium storage capacity. A battery is a combination of one or more electronic cells connected to electrical energy. The basic components of a conducting cell such as a lead-acid cell are a fine electrode, without an electrode, a porous separator and an electrolyte. During cellular activity, ions are formed and consumed in the electrode / electrolyte coupling visible by oxidation / reduction. An electrolyte, in a can, that is a liquid or gaseous substance, has a high ion flow but not electricity, because if the electrolyte holds the electrolyte the battery will flows itself. Eliminates internal circulation between electrolyte electrodes. In Figure.8 a similar battery model of Thevenin was introduced.

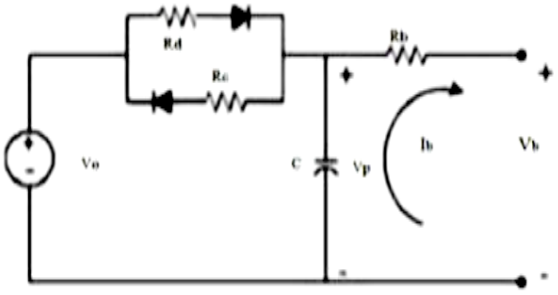

Fig 8: Thevenin equivalent battery model

The open circuit voltage is denoted as R_c, the internal air capacitor is denoted as R_d and the final voltage are denoted as R_b, and C is the polarization power of the battery. The current ia is considered positive if it pulls out and has a gateway alternative. The regional model statistics are:

$$V_p = \frac{1}{C}\left[\frac{V_0 - V_a}{R_d} - I_b\right] \quad (8)$$

$$V_b = V_p - I_b R_b \quad (9)$$

III. Unified Power Quality Controller (UPQC)

UPQC is one of the FACTS integration devices, it has no additional storage or power equipment, but can be simultaneously effective and efficient compensation function, and can be seen in robust quick fixes across power systems, such as voltage, impedance, phase and power parameters, to improve system stability. of power. The UPQC system architecture diagram, as shown in Figure 9, mainly including the main circuit and the control circuit, the main circuit consists of two systems connecting the V_{SC1} converter with transformer T_1 to the same systems and the V_{SC2} converter using transformer T_2 series systems, connectors the medium is constructed by DC power, its capacitance value is large, to ensure that the power supply is not large, so under the constant state of operation of the state, both limit capacitance C is fundamental, its action is similar to DC power; The control circuit is made up of a control module and a set of parameters, usually used to turn off the thyristor control, in adjusting the different control Angle, respectively, to control serial-to-parallel converter output voltage, to achieve the system control power and power.

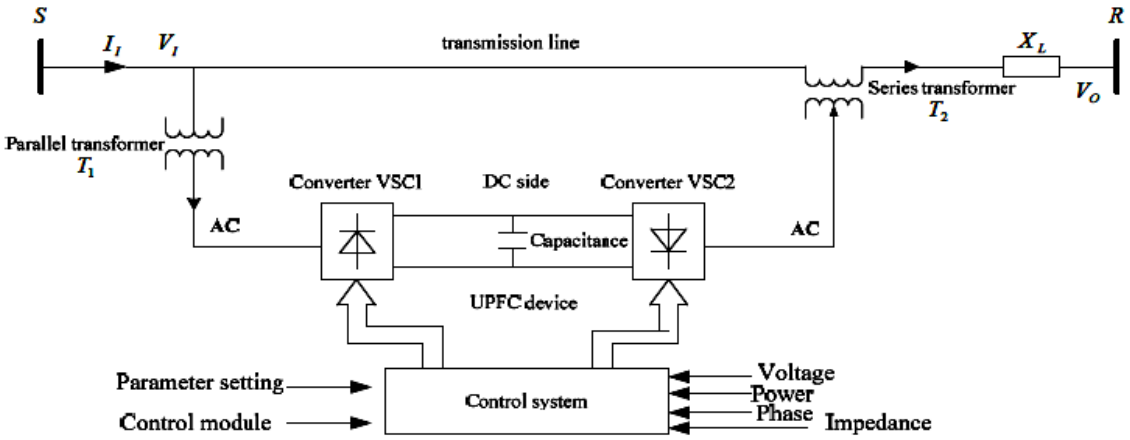

Figure 9The structure diagram of the UPQC

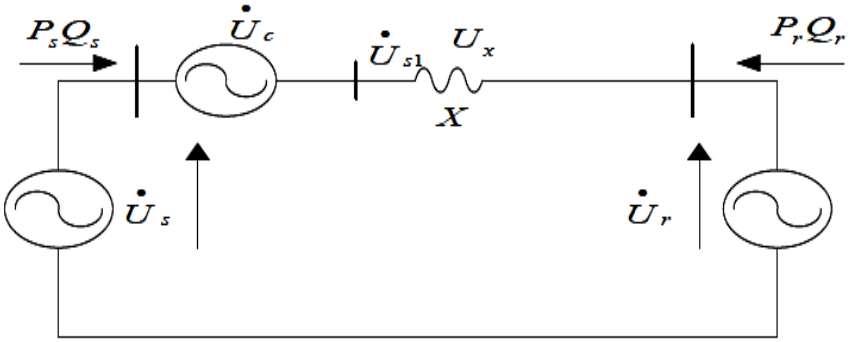

Figure 10: Equivalent circuit of the UPQC

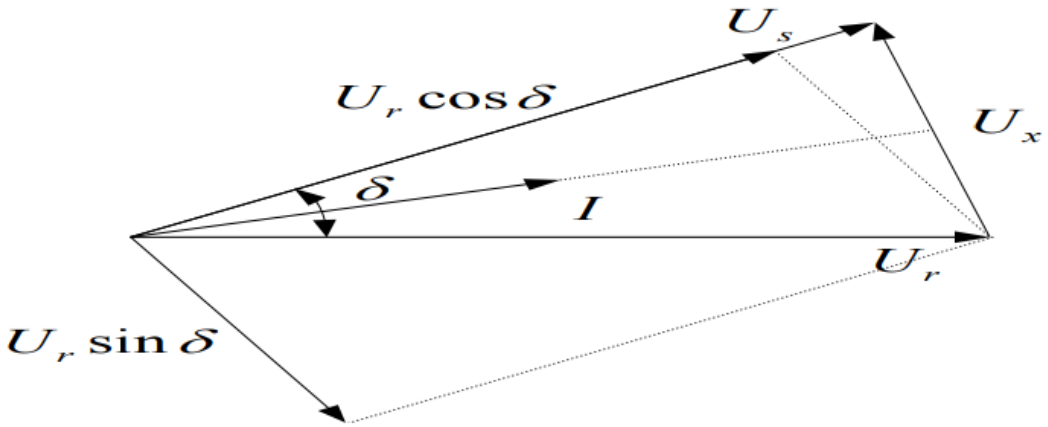

Figure 11: Vector diagram of UPQC

To demonstrate the functionality of the UPQC features, to present the UPQC power system diagram and the vector diagram as shown in Figure 10 and the UPQC vector are shown in Figure 11, It should now be considered that the simple redesign of the transmission line is X. Transmission to vector voltage is U_s, and reception at vector voltage is $\dot{U}_r$, respectively; δ is the angle of the transmission line; P_s, $Q_s$and P_r, Q_r are active forces and active forces by sending and receiving respectively.

From the above the numbers take $\dot{U}_s$as a reference vector, namely:

$$\dot{U}_s = \dot{U}_s e^{j0} = U_s \tag{10}$$

$$\dot{U}_r = \dot{U}_r e^{-j\delta} = U_r(cos\delta - jsin\delta) \tag{11}$$

Therefore find the end of active energy and active energy can be counted as follows:

$$P_r + jQ_r = \dot{U}_r \left(\frac{\dot{U}_s - \dot{U}_r}{jX}\right)^* = U_r(cos\delta - jsin\delta)\left(\frac{U_s - U_r cos\delta + U_r jsin\delta}{jX}\right)^* \tag{12}$$

Enter formula (11) in formula (12).

$$P_r + jQ_r = \dot{U}_r \left(\frac{\dot{U}_s - \dot{U}_r}{jX}\right)^* = \frac{U_r}{X}(cos\delta - jsin\delta)(jU_s - jU_r cos\delta + U_r jsin\delta) \tag{13}$$

$$= \frac{U_r U_s sin\delta}{X} - j\frac{U_r(U_r - U_s cos\delta)}{X} \tag{14}$$

In the same way, bringing the end of active energy and active energy can be calculated as follows:

$$P_r + jQ_r, -\dot{U}, \left(\frac{\dot{U}, -\dot{U}}{jX}\right)^* \tag{15}$$

Finally complete the formula, namely:

$$P_r + jQ_r = \dot{U}_s \left(\frac{\dot{U}_s - \dot{U}_r}{jX}\right)^* = \frac{U_s}{X}(jU_s - jU_r cos\delta + U_r jsin\delta) = \frac{U_r U_s sin\delta}{X} + j\frac{U_r(U_r - U_s cos\delta)}{X} \tag{16}$$

Comparative formula (13) and formula (16), where you ignore the active line loss, however the similarity between finding the end and bringing the end to the active force, namely:

$$P = P_s = P_r = \frac{U_r U_s sin\delta}{X} \tag{17}$$

Thus the two ends of the active force can be shown respectively as follows:

$$Q_r = -\frac{U_r(U_r - U_s cos\delta)}{X}, Q_s = \frac{U_s(U_s - U_r cos\delta)}{X} \tag{18}$$

If $U_s = U_r = U$, so we can get:

$$P = P_s = P_r = \frac{U^2 sin\delta}{X}, Q_s = -Q_r = \frac{U^2(1-cos\delta)}{X} \quad (19)$$

and if $U_s = U_r = U = 1, X = 1$, at last we can get:

$$P = P_s = P_r = sin\delta, Q_s = -Q_r = (1 - cos\delta) \quad (20)$$

According to the above formula, in order to adjust the power transmission, we can adjust the following parameters, such as voltage amplitudes U_r at the end of the receiver, voltage amplitudes U_s at the end of delivery, reaction X and line transfer angle δ if, if two limits of voltage value and -reaction reaction under continuous conditions, we can change the Angle, so it has a great value for good system performance.

IV. Overview of Optimization techniques

The problem with optimization is the problem of finding the best solution possible. In this paper Lightning Search Algorithm and UPQC are proposed to solve PQ problems in the HRES system. This controller works mainly on two different control strategies such as the active power filter and the shunt power series. Suggested existing algorithms are Harris Hawks Optimizer, Gray Wolf Optimization and Modified Particle Swarm Optimization.

Modified Particle Swarm Optimization (MPSO)

PSO is the simplest and most popular. In this way, multiple permissions are allowed to move into the search area with multiple values [J. Kennedy, 1995]. Each particle speed will be updated during the search:

$$v_i^{k+1} = \omega v_i^k + c_1 rand_1\left(P_{i,pbest}^k - x_i^k\right) + c_2 rand_2\left(P_{i,gbest}^k - x_i^k\right) \quad (21)$$

When initial weight is ω which is varies between 0.4 to 0.9, random selection $rand_1$ and r_2 varies in range [0, 1] and c_1 and c_2 are the acceleration coefficients are. The position of the crowd is revived by

$$x_i^{new} = x_i + v_i \quad (22)$$

With more iteration, the best solution can be found by

$$x_i^{k+1} = \left\{\frac{x_{i,new} iff\left(x_{i,new}\right) \leq f(x_i)}{x_i \; Otherwise}\right\} \quad (23)$$

GWO (Grey Wolfs Optimization) Technique

This GWO is a new metaheuristic process based on Grey-Wolf-minded mob tactics while hunting deer [S. United States, 2014]. Gray wolves live in pockets and are placed in a state of hunting. To model the hunt, the best solutions are given to α wolf after groups' β, γ and δ. The wolf formed a circle around the victim to begin hunting for the victim, which was given to

$$\vec{D} = \left|\vec{C}\overrightarrow{X_p} - \vec{A}\vec{X}(t)\right| \quad (24)$$

$$\vec{X}\,(t+1) = \vec{X}_p(t) - \vec{A}\vec{D} \quad (25)$$

In equation (25) 't' stands for current multiplication. The X and X_P carriers represent the location of the gray wolf and the victim, respectively, where A and C are equally distributed carrier given in Equation (26) and (27).

$$\vec{A} = 2.\vec{a}\overrightarrow{r_1} - \vec{a} \quad (26)$$

$$\vec{C} = 2.\overrightarrow{r_2} \quad (27)$$

In equations (26) - (27), r_1 and r_2 represent a random vector that varies in [0, 1] and the 'a' fraction decreases from 2 to 0 during multiplication. The process of hunting can be done as

$$\vec{D}_\propto = \left|\vec{C}_1\vec{X}_\propto - \vec{X}\right| \quad (28)$$

$$\vec{D}_\beta = \left|\vec{C}_2\vec{X}_\beta - \vec{X}\right| \quad (29)$$

$$\vec{D}_\delta = \left|\vec{C}_3\vec{X}_\delta - \vec{X}\right| \quad (30)$$

$$\overrightarrow{X_1} = \vec{X}_\propto - A_1(\vec{D}_\propto) \quad (31)$$

$$\overrightarrow{X_2} = \vec{X}_\beta - A_2(\vec{D}_\beta) \quad (32)$$

$$\overrightarrow{X_3} = \vec{X}_\delta - A_3(\vec{D}_\delta) \quad (33)$$

The limited number of wolf positions α, β and δ are found to be the best plunder positions given as

$$\overrightarrow{X_{(t+1)}} = \frac{\overrightarrow{X_1}+\overrightarrow{X_2}+\overrightarrow{X_3}}{3} \quad (34)$$

Whale Optimization Algorithm (WOA)

WOA is a new way of doing things as they are one of the most intelligent animals as their brains contain certain cells that are common to human brain cells [K. S. Latha, 2014; H. Le-Huy, 2009]. In the WOA, search agents have revived the position in each iteration and the work objectives were determined based on this review. The process is repeated until the maximum number of repetitions and the best solutions are maintained.

At first, the whales go straight to their prey and then surround the prey. First, the WOA calculation is expected to have a current solution as the closest and most effective solution. When a good solution is found, other whales (search operators) will try to update their positions in terms of better order. The statistical introduction of whales around the diet can be defined as:

$$\vec{H} = \left|\vec{E}\overrightarrow{Y^P}(i) - \vec{Y}(i)\right| \quad \textbf{(35)}$$

$$\vec{Y}(i+1) = \overrightarrow{Y^P}(i) - \vec{D}.\vec{H} \quad \textbf{(36)}$$

where I show the current multiplication, $\vec{Y}$ is the vector of the current resolution of the available solution and $\overrightarrow{Y^P}$ is the vector of the best position.

The D and $\vec{E}$ are two vector coefficients determines as:

$$\vec{E} = 2r_2 \quad \textbf{(37)}$$

$$\vec{D} = 2\vec{d}r_1 - \vec{d} \quad \textbf{(38)}$$

The values of D are reduced from 2 to 0, $\vec{D}$ vector ranges from $[-\vec{d}, \vec{d}]$**.** Both random values r_1 and r_2 bring the values between 0 and 1.

In this bubble-net follow-up step, two types of models are defined, reducing the rotation path and the regeneration zone. The attitude of shrinking whales is made by reducing the number of $\vec{d}$. The second method is based on emotional rejuvenation and can be described as:

$$\vec{Y}(i+1) = \overrightarrow{F'}b_{el}(2\pi r) + \overrightarrow{Y^P}(i) \quad \textbf{(39)}$$

During the chase, the whales simultaneously swim around the deer in the two previously mentioned techniques. To rehabilitate whales, 50% of the following strategies are considered:

$$\vec{Y}(it+1) = \begin{cases} \overrightarrow{Y^P}(i) - \vec{D}.\vec{H} & p < 0.5 \\ \overrightarrow{F'}b_{el}(2\pi r) + \overrightarrow{Y^P}(i) & p \geq 0.5 \end{cases} \quad \textbf{(40)}$$

Where $\overrightarrow{F'}$ indicates the best position between prey and whale.

Search action depends on men for vector variations. Depending on the position of each other, humpback whales look for the best position. To get the right position all over the world,

$$\vec{F} = \left|\vec{D}.\overrightarrow{Y^{rand}} - \vec{Y}(i)\right| \quad \textbf{(41)}$$

$$\vec{Y}(i+1) = \left|\overrightarrow{Y^{rand}} - \vec{D}.\vec{H}\right| \quad \textbf{(42)}$$

Where $\overrightarrow{Y^{rand}}$ a random vector position whale chosen from the current population.

Harris Hawks Algorithm (HHO)

Harris hawk is one of the most intelligent and outstanding hunting birds of prey in nature that demonstrates the power of following along, circling, taking out and trapping a potential animals (rabbit) in food groups. Here, the first population is considered to be the group of rabbits that have been planned (solution of performance) from a variety of indicators using seven kill or shock techniques. At first, the hawk leader tried to kill him the victim; if it fails to catch an animal due to the victim's aggressive behavior and escape behavior, change strategies followed, became another team member (eagle in group) can beat the surviving victim and catch him. The advantage of this collaboration is that the birds were able to follow the rabbits identified by the confusion and weakness of the fleeing animals. At HHO, the competition between the contestants is the Harris Hawks and the best / international solution has been targeted [Heidari, A.A, 2019].

Step1—**Exploration phase:** Harris hawks roughly perch and wait elsewhere, watching and monitoring the victim's attack. The leader of the hawks perch depending on Status and robbery of family members. This is illustrated in the context of the mathematical equation for changing the distance (q) between the unit and the spool as follows:

$$X(i+1) = \begin{cases} X_{rand}(i) - r_1 X_{rand}(t) - 2r_2 X(i) & q \geq 0.5 \\ X_r(i) - X_m(i) - r_3(LB + r_4(UB - LB) & q < 0.5 \end{cases} \quad (43)$$

where the hawk's regenerative vector is X (t + 1) in the iteration of i+1,

where X (t + 1) is the hawk's regenerative vector in the i+1 iteration, $X_r(t)$ is the feed, hawk position vector is X(t), random numbers r_1, r_2, r_3, r_4, and q in the range of (0,1), Upper and Lower bound variables are UB and LB, while $X_r(t)$ and $X_m(t)$ are the first random deliberation. Each hawk average position is defined as

$$X_{i+1}(t) = \frac{1}{N}\sum_{i=1}^{N} X_i(t) \quad (44)$$

where the hawks current position is X_i (t), the vector refresh area is X_i + 1 (t), and N is the total number of hawks.

Step2: During the search, the hawks try to find places and defeat the attacker. As a result there is a change in the value of the energy (E) of the animal and it is derived from:

$$Escaping\ Energy\ E = 2E_0\left(1 - \frac{t}{T}\right) \quad (45)$$

where the maximum iteration count is denoted as T, the current iteration is stated as t, and the initial intensity (E_0) fluctuates randomly linking (−1 to 1) in all recurrences. E ≥ 1 indicates the success of the victim's connection and the hawks are looking for the victim elsewhere, E <1 represents that the victim is tired and the hawk became more aggressive with a surprising beating who make exploitation phase a solution.

Step 3—Exploitation phase: In this stage, change strategies follow the attack on the victim. The victim always escapes the hawk, and the chance to escape the deer is shown as r. When r <0.5 the victim can escape, and in flipside when r ≥ 0.5 the probability of escape can fail. Either way, the hawk will attack the prey and will succeed or not with a soft or hard circle. If the victim escapes from there (r ≥ 0.5) and | E | <0.5 then severe siege. Conversely, if (r ≥ 0.5) is not | E | ≥ 0.5, then there is a soft siege. Here, r is denoted possible for the victim to escape. It can be simulated in the following mathematical way

Step 4—Soft siege: Here, the rabbit is really strong and tries to jump by jumping while the hawks walks around a bit, which is like

$$X(t+1) = \Delta X(t) - E|JX_{rabbit}(t) - X(t)| \quad (46)$$

$$\Delta X(t) = X_{rabbit}(t) - X(t) \quad (47)$$

Random rabbit jump is given by J = 2(1 − r_5), where the ΔX(t) the difference between the position vector of successive repetitions and the random number r5 is in the range (0.1)

Step 5—Hard siege: In this case, the deer ended up very tired and the hawks are circling around hard and performing amazing feats. Positions are renewed using (45) as provided by

$$X(t+1) = X_{rabbit}(t) - E|\Delta X(t)| \quad (48)$$

Step 6—Soft siege with continuous rapid dives: The rabbit is still strong and trying to escape, and this is described as | E | ≥ 0.5 and r <0.5, and more sieges before being attacked by consumers by surprise. This step is smarter than the previous case.

The rabbit is still strong and trying to escape, and this is portrayed as | E | ≥ 0.5 and r <0.5, and more siege is required before a surprise attack by consumers. This move is much smarter than the previous case.

Here the idea of Levy flights is introduced so that the hawks could move forward faster to make a softer siege and the following movements of the victim were tested by the unit using the following equations:

$$Y = X(t) - E|JX_{rabbit}(t) - X(t)| \quad (49)$$

Despite several attempts, the Hawks compared their own moves to previous dives, to see if the dive was good or not. When diving is irrational, it makes for unusual, sudden and quick immersion in a carnivorous animal. Therefore, the final law to restore the Hawks' position in the soft siege category is:

$$X(t+1) = \begin{cases} Y \ if \ F(Y) < F(X(t)) \\ Z \ \ if \ \ F(Z) < F(X(t)) \end{cases} \quad (50)$$

Step 7—Hard siege with continuous rapid dives: In this regard, | E | <0.5, tired and exhausted carnivores. The siege of the heavy use by the Hawk and reduce the distance to the region since the winter season.

LSA (Lightning Search Algorithm)

LSA is used, like many metamorphic algorithms, to solve complex nonlinear problems. The LSA-driven lightning system uses a step-by-step distribution system that looks at particles called projectiles in building a one-step leader wood structure and the next two leader tips. The first step leader of the people created by the propeller transformer can be made from 3 types of propellants, namely space rocket, robot modification and advanced projectiles [H.Shareef, AA, 2015].

Transition Projectile: The first phase is the formation of action leaders due to the unplanned missile launch of the shift. It can be formatted as a random number using the same distribution possibilities.

$$f(x^T) = \begin{cases} \frac{1}{b-a} \ for \ a \le x^T \le b \\ 0 \quad elsewhere \end{cases} \quad (51)$$

Where the initial tip energy of the step leader is denoted as x^T. The step leaders is denoted as SL, for a population N, is given as $sl_1, sl_2, sl_3, \dots\dots, sl_N$, N random projectiles $[P^T = P^{T_1}, P^{T_2}, P^{T_3}, \dots, P^{T_N}]$ that satisfy the required solution dimension.

Space Projectile: The space Projectile seeks to find the leading leaders by empowering the regional leaders of the previous leaders in Step + 1 as step leaders are transformed after N.

Space projectile p^S position = $[P^{s_1}, P^{s_2}, P^{s_3}, \dots, P^{s_N}]$ using the descriptive distribution parameter of form μ in step + 1 can be partially modeled as a random number.

$$f(x^s) = \begin{cases} \frac{1}{\mu} e^{(\frac{-x^s}{\mu})} \ for \ x^s \ge 0 \\ 0 \quad for \ x^s \le 0 \end{cases} \quad (52)$$

Therefore, the $[P^{s_i}$ at step + 1 is represented by:

$$p^s_{i-New} = p^s_i \pm exprand(\mu_i) \quad (53)$$

Lead Projectile: the leader's moving motion is very close to the ground, its related projectile does not have enough power to open large parts before the moving tip. This makes it possible to model the implementation of the numbers obtained from the distribution models.

$$f(x^L) = \frac{1}{\sigma\sqrt{2\pi}} e^{\frac{(-x^L-\mu)^2}{2\sigma^2}} \quad (54)$$

The equation demonstrates that a lead projector randomly generated using a form (μ) parameter can examine all indications from the current state of a lead projector with the control capability represented by the parameter (σ) parameter.

p^L in step + 1 can be defined as:

$$p_l^{new} = p^L + normrand(\mu_L, \mu_\sigma) \quad (55)$$

normrand represents a random number generated from a standard distribution function.

Implementation of LSA for the Hybrid Renewable energy system

Finding the right amounts of heavy objects is usually done using artistic data. In this function, the defined error is used as the object function, defined as:

$$Minimize \ F = \sqrt{\frac{\sum_{k=1}^{N}\left[p_k^{observed} - p_k^{forecasted}\right]^2}{\sum_{k=1}^{N}\left[p_k^{observed}\right]^2}} * 100\% \quad (56)$$

when N defines the amount of artistic detail, $p_k^{observed}$ recognized the power of HERS in kth recognition, and $p_k^{forecasted}$ the predicted power at k^{th} output times in the optimization process.

V. Simulation Results and Discussion

This section reports simulation results and discusses power control in hybrid and UPQC renewable energy sources using the proposed strategy. In the Matrix Laboratory / Simulink platform, the proposed process is being implemented. The effect of the proposed strategies and existing strategies is analyzed. Existing strategies include base, Modified particle swarm optimization, gray wolf optimizer, Whale Optimization technique and Harris Hawks Optimization.

PV and WT frames are considered the source of the framework. In this case study, the basic parameters of PV and WT irradiance and wind speed are adjusted as a steady level as the control characteristics of the control structure. PV radiation conditions are considered to be 1000W / m2. Identified by the degree of irradiance of PV, the strength is made by the frame used to leak the mass application. WT speed is considered 12m / s, due to WT power generation speed. Therefore, HRES has produced the necessary capacity to meet high demand and reduce PQ issues. The battery is also associated with a frame that is powered by only the basic foundations of the PV and WT energy frames.

Figure 12 is a present simulation of a hybrid connected grid system consisting of solar power, wind power and resources and controlled by a voltage regulator. To improve the power quality of the device connected to the hybrid system UPQC device is used. Solar radiation, wind speed and Battery power are considered as implants. Figure 13 shows the model below the hybrid system. The Grid-connected Hybrid system is used for 0.5sec in the MATLAB / Simulink software.

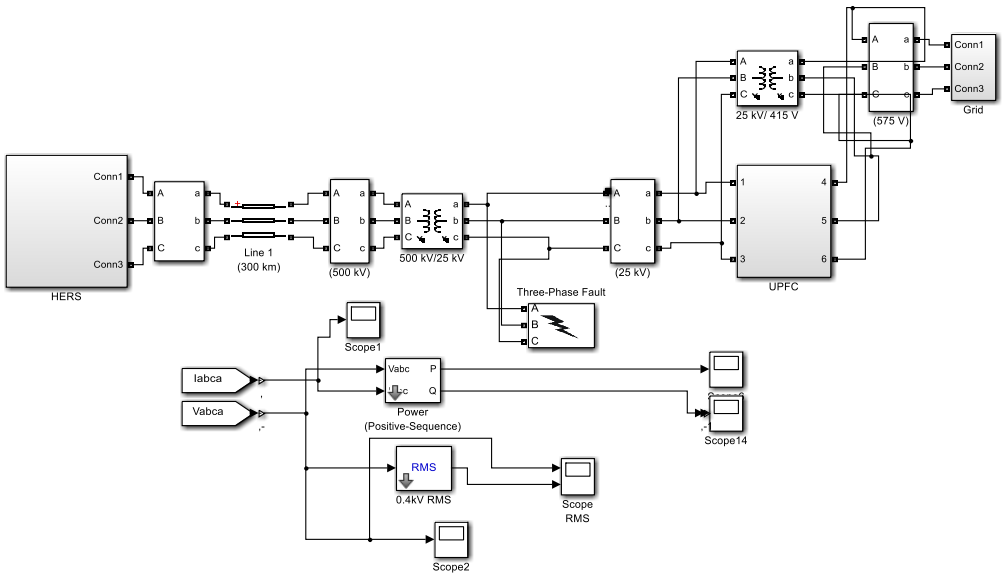

Figure 12: Simulation of grid connected Hybrid system using UPQC controller

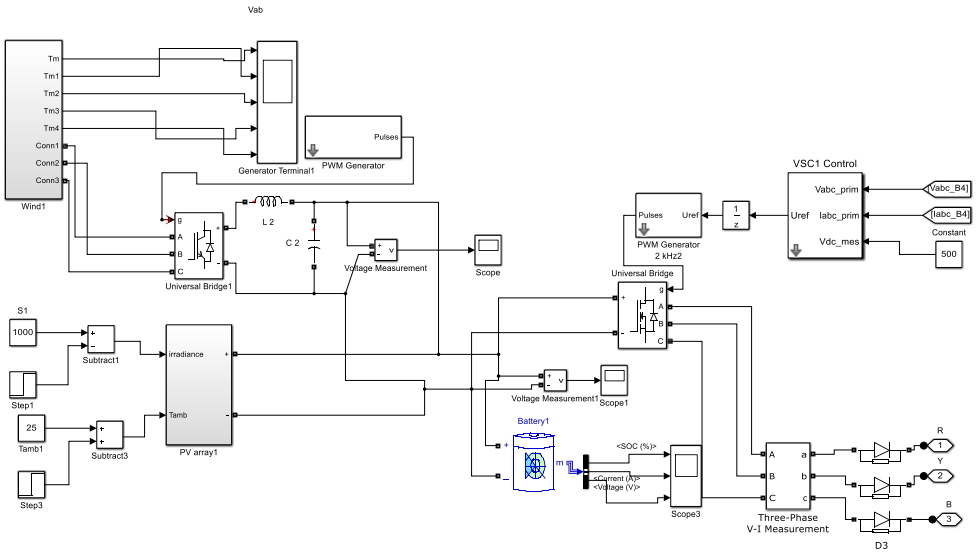

Figure 13: Subsystem Modeling of Hybrid System

Photovoltaic System

The 410 watts Solar Photovoltaic Panel is modeled on this paper according to the electrical features of the panels that provide information on the operating condition of the system. The input value of the irradiance is maintained at 1000W / m^2 and the reference temperature is at 25^0c and it is due to the electrical voltage and current shown in Figure 14 and Figure 15 showing the P-V and I-V features of the photovoltaic system. In this model 144 PV cells are connected in series. Each cell provides 0.7V. The total output voltage obtained is 82V. The total current generated by the PV system is 5A.

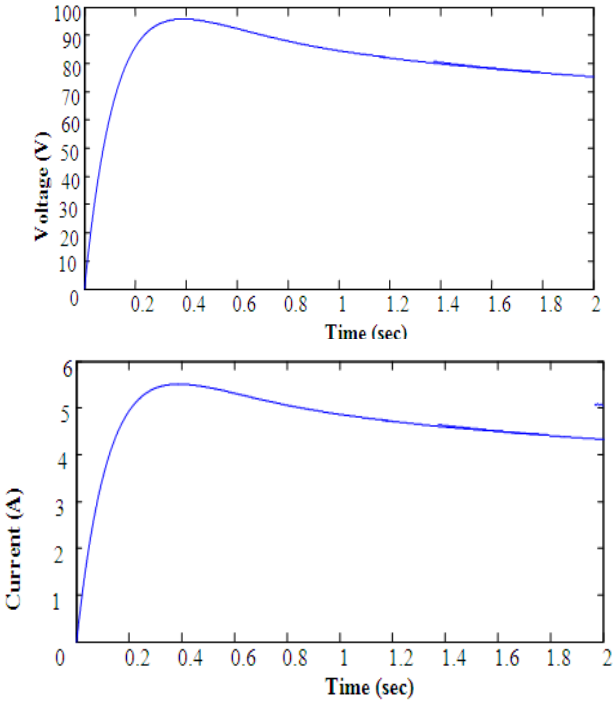

Figure 14: Voltage and current of the Solar/PV

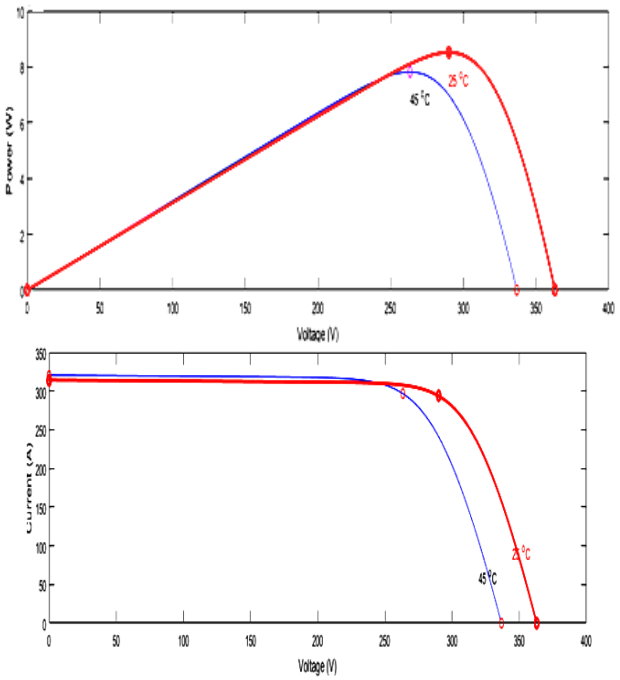

Figure 15: P-V and I-V characteristics of solar/PV

Wind Turbine Characteristics:

At a speed of about 12m / s the installation of the wind power supply system and the resulting speed, voltage and current are plotted which is shown in Figure 16. For the wind turbine system speed to be about 12m / s the following features such as power output were achieved at 45V and the current output is 12A.

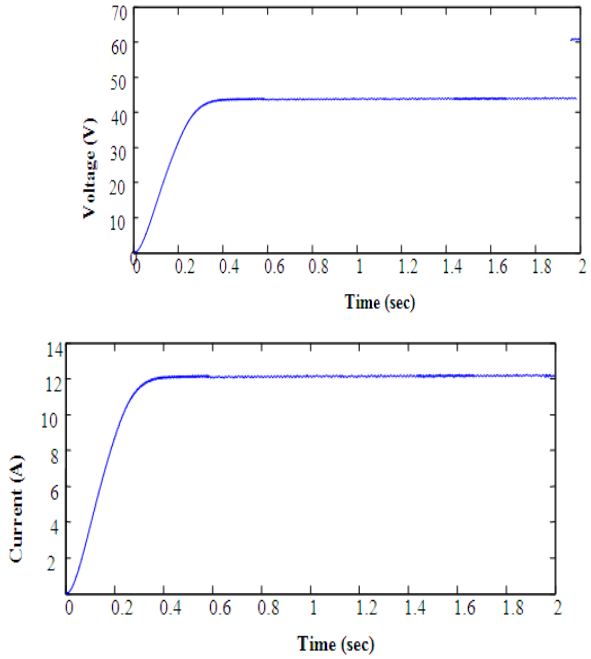

Figure 16: Voltage and current of the wind

Control Algorithm:

There are two operating modes, in the First mode grid is connected to loads that do not have a problem with the quality of power example voltage sag, Current sag, real power active power is guaranteed without UPQC control. The 3phase, 50HZ, 415V, supply line can be connected to more than one load, that is, due to the increase in load or due to a situation that has occurred on the distribution side, the power supply is distorted; this

can be reduced with the help of UPQC. In this paper, an increase in load or fault occurs in the range of 0.08 sec to 0.15 msec. At that time, UPQC is active and inactive for the remainder of the term. By using controls, when a fault occurs or an increase in the load provides error signal of a pulse generator that generates pulses for the Voltage source inverter that injects a three-phase power outlet from the distribution line with an injection transformer. In this case there are three cases. The three cases are three phase fault compensation, Line to Line fault compensation, Single Line to Ground Fault Compensation and Double Line to Ground Fault Compensation.

Case 1: Three phase fault compensation

A three-phase fault occurred at 0.08s and the voltage in all the three phases is dipped to 190V (70% sag) for using Modified Particle Swarm Optimization algorithm, 210V (50%sag) for using Grey wolf algorithm, 310 (30% sag) V for using Whale optimization algorithm, 390V (10% sag) for Harris Hawks Algorithm and 413V (3% sag) for Lightning search algorithm. UPQC is activated at 0.08s and it injects a voltage of 210V for MPSO, 192V for GWO, 101V for WOA, 22V for HHO and 2V for LSA in all the three phases. Load voltage is not compensated to 415V for using MPSO, GWO, WOA and HHO is shown in Figure 17 (a), Figure 17(b), Figure 17(c) and Figure 17(d). The Proposed LSA clearly compensates the sag voltage is 415V and the UPQC injected voltage is 2V, which is shown in Figure 17 (e).

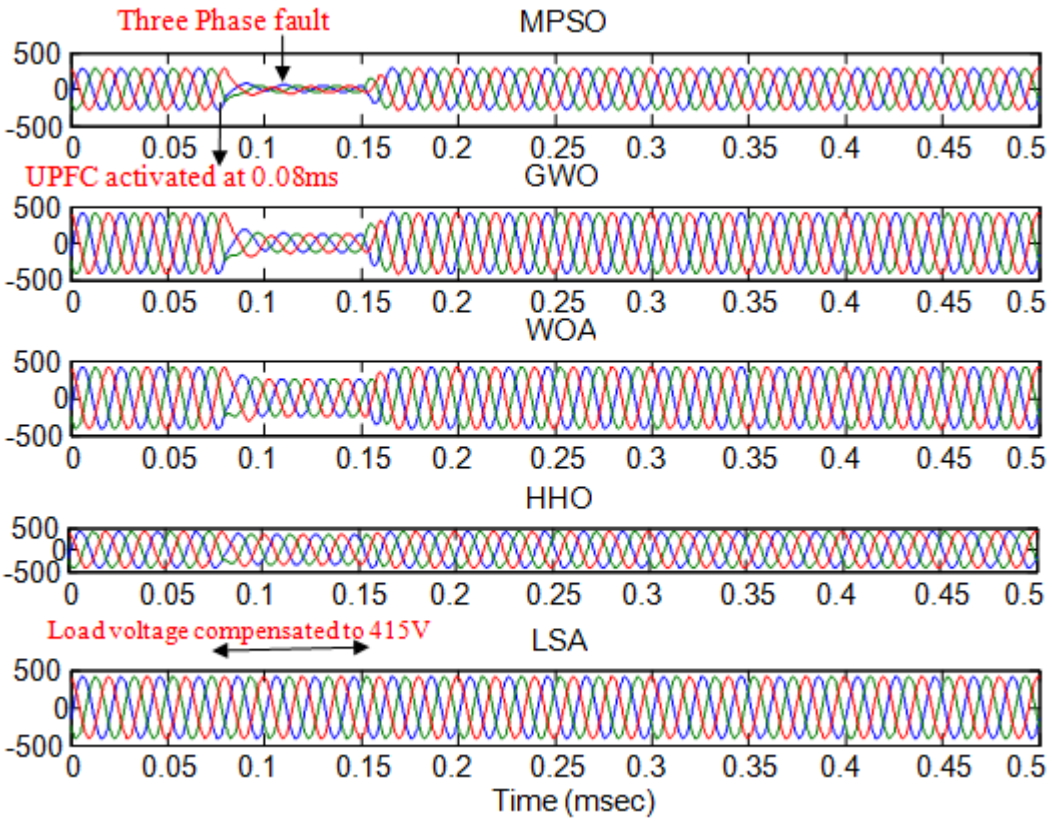

Figure 17: Three phase fault voltage sag compensation of using MPSO, GWO, WOA, HHO and LSA techniques

A three-phase fault occurred at 0.08s and the current in all the three phases is dipped to 5A (70% sag) for using Modified particle Swarm Optimization algorithm, 9A (50%sag) for using Grey wolf algorithm, 11A (20% sag) V for using Whale optimization algorithm, 18A (10% sag) for Harris Hawks Algorithm and 22A (1% sag) for Lightning search algorithm. UPQC is activated at 0.08s and it injects a current of 19A for MPSO, 13A for GWO, 11A for WOA, 9A for HHO and 3A for LSA in all the three phases. Load current is not compensated to 25A for using MPSO, GWO, WOA and HHO is shown in Figure 18 (a), Figure 18(b), Figure 18(c) and Figure 18(d). The Proposed LSA clearly compensates the sag voltage is 25A and the UPQC injected current is 3A, which is shown in Figure 18 (e).

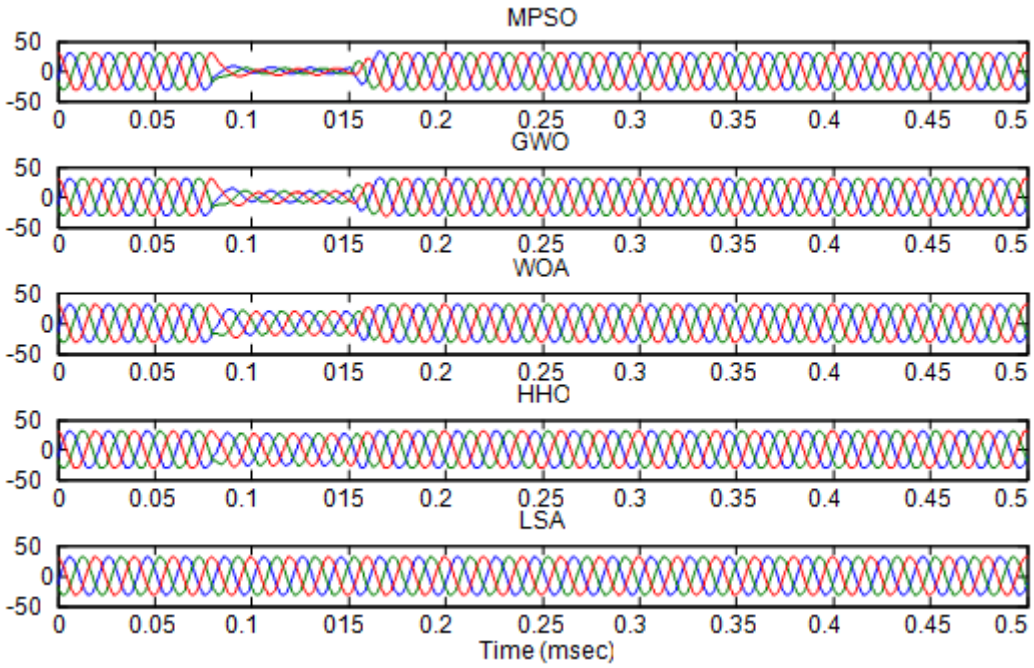

Figure 18: Three phase fault current sag Compensation of using MPSO, GWO, WOA, HHO and LSA techniques

Case 2: Line to Line fault compensation

A Line to line fault occurred at 0.08s and the voltage in the A phase is dipped to 90V (80% sag) and B phase is dipped to 110(75% sag) for using Modified particle Swarm Optimization algorithm, A phase is dipped to 180V (60%sag) and B phase is dipped to 190V (45%sag) for using Grey wolf algorithm, A phase is dipped to 320 V (30% sag) and B phase is dipped to 330V (25% sag) for using Whale optimization algorithm, A phase is dipped to 395V (10% sag) and B phase is dipped to 405V (5% sag) for Harris Hawks Algorithm and A phase is dipped to 412V (3% sag) and B phase is dipped to 413V (2% sag) for Lightning search algorithm. UPQC is activated at 0.08s and it injects a voltage of A phase is 320V and B phase is 300V for MPSO, A phase is 230V and B phase is 220V for GWO, A phase is 80V and B phase is 70V for WOA, A phase is 18V and B phase is 9V for HHO and A phase is 3V and B phase is 2V for LSA in all the three phases. Load voltage is not compensated to 415V for using MPSO, GWO, WOA and HHO is shown in Figure 19 (a), Figure 19(b), Figure 19(c) and Figure 19 (d). The Proposed LSA clearly compensates the sag voltage is 415V and the UPQC injected voltage of A phase is 3V and B phase is 2V, which is shown in Figure 19 (e).

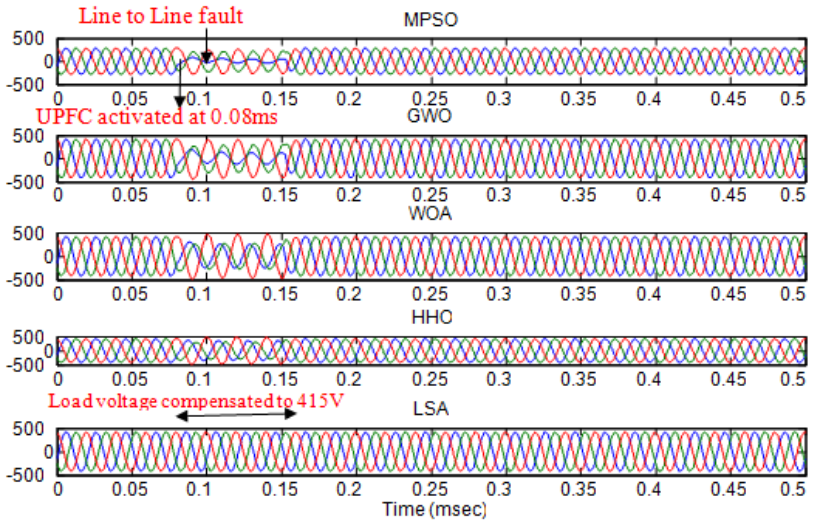

Figure 19: Line to Line fault Voltage sag Compensation of using MPSO, GWO, WOA, HHO and LSA techniques

A Line to line fault occurred at 0.08s and the current in the A phase is dipped to 5A (85% sag) and B phase is dipped to 6A (80% sag) for using Modified particle Swarm Optimization algorithm, A phase is dipped to 10A (60%sag) and B phase is dipped to 12A (50%sag) for using Grey wolf algorithm, A phase is dipped to 16A (40% sag) and B phase is dipped to 18A (30% sag) for using Whale optimization algorithm, A phase is dipped to 19A (18% sag) and B phase is dipped to 21A (10% sag) for Harris Hawks Algorithm and A phase is dipped to 22A (5% sag) and B phase is dipped to 24A (3% sag) for Lightning search algorithm. UPQC is activated at 0.08s and it injects a voltage of A phase is 18A and B phase is 17V for MPSO, A phase is 14A and B phase is 12A for GWO, A phase is 9A and B phase is 7A for WOA, A phase is 5A and B phase is 4A for HHO and A phase is 3A and B phase is 1A for LSA in all the three phases. Load current is not compensated to 25A for using MPSO, GWO, WOA and HHO is shown in Figure 20(a), Figure 20(b), Figure 20(c) and Figure 20 (d). The Proposed LSA clearly compensates the sag voltage is 25A and the UPQC injected current of A phase is 3A and B phase is 1A, which is shown in Figure 20 (e).

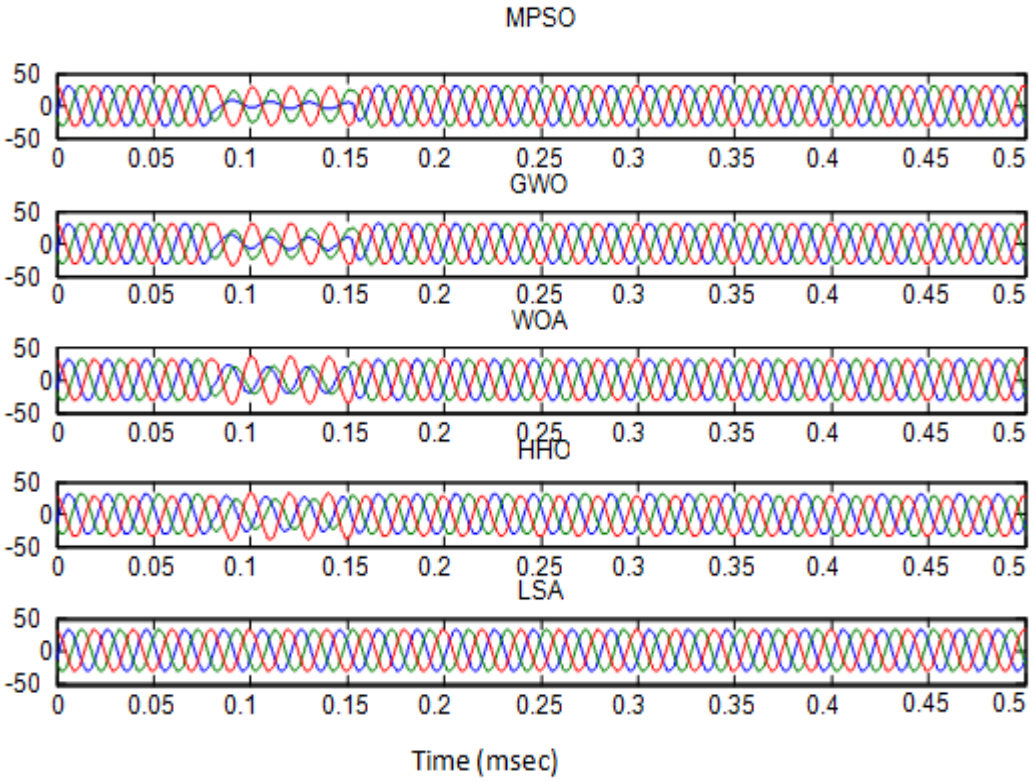

Figure 20: Line to Line fault current sag Compensation of using MPSO, GWO, WOA, HHO and LSA techniques

Case 3: Single Line to Ground Fault Compensation

A Single Line to Ground fault occurred at 0.08s and the voltage in the A phase is dipped to 120V (60% sag) from 415V in phase A for using Modified particle Swarm Optimization algorithm, A phase is dipped to 200V (50%sag) for using Grey wolf algorithm, A phase is dipped to 280 V (40% sag) for using Whale optimization algorithm, A phase is dipped to 395V (10% sag) for Harris Hawks Algorithm and A phase is dipped to 405V (6% sag) for Lightning search algorithm. UPQC is activated at 0.08s and it injects a voltage of A phase is 290V for MPSO, A phase is 195V for GWO, A phase is 130V and for WOA, A phase is 18V for HHO and A phase is 10V for LSA in all the three phases. Load voltage is not compensated to 415V for using MPSO, GWO, WOA and HHO is shown in Figure 21 (a), Figure 21(b), Figure 21(c) and Figure 20 (d). The Proposed LSA clearly compensates the sag voltage is 415V and the UPQC injected voltage is 10V, which is shown in Figure 21(e).

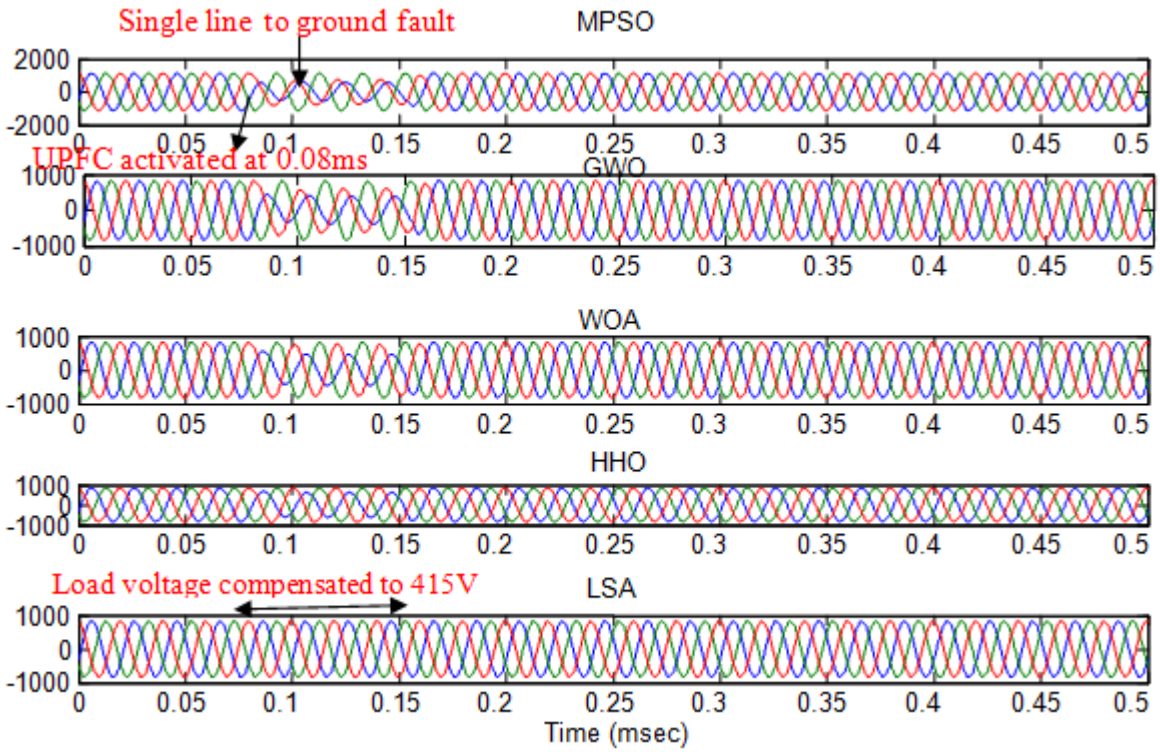

Figure 21: Single line to ground fault voltage sag Compensation of using MPSO, GWO, WOA, HHO and LSA techniques

A Single Line to Ground fault occurred at 0.08s and the current in the A phase is dipped to 7A (60% sag) from 25A in phase A for using Modified particle Swarm Optimization algorithm, A phase is dipped to 10A (53%sag) for using Grey wolf algorithm, A phase is dipped to 14 A (45% sag) for using Whale optimization algorithm, A phase is dipped to 19 (25% sag) for Harris Hawks Algorithm and A phase is dipped to 22A (5% sag) for Lightning search algorithm. UPQC is activated at 0.08s and it injects a voltage of A phase is 17A for MPSO, A phase is 14A for GWO, A phase is 10A and for WOA, A phase is 5A for HHO and A phase is 3A for LSA in all the three phases. Load voltage is not compensated to 25A for using MPSO, GWO, WOA and HHO is shown in Figure 22 (a), Figure 22(b), Figure 22(c) and Figure 22 (d). The Proposed LSA clearly compensates the sag voltage is 25A and the UPQC injected current is 3A, which is shown in Figure 22 (e).

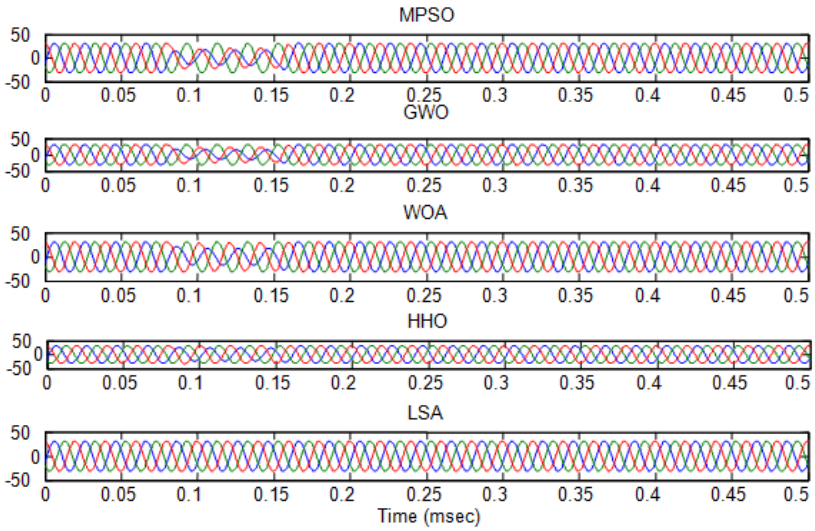

Figure 22: Single line to ground fault current sag Compensation of using MPSO, GWO, WOA, HHO and LSA techniques

Case 4: Double Line to Ground Fault Compensation

A Line to line fault occurred at 0.08s and the voltage in the phase A is dipped to 95V (80% sag) and phase B is dipped to 113 (75% sag) for using Modified particle Swarm Optimization algorithm, phase A is dipped to 185V (60%sag) and phase B is dipped to 190V (45%sag) for using Grey wolf algorithm, phase A is dipped to 315V (30% sag) and phase B is dipped to 320V (25% sag) for using Whale optimization algorithm, phase A is dipped to 390V (10% sag) and phase B is dipped to 395V (5% sag) for Harris Hawks Algorithm and phase A is dipped to 413V (2% sag) and phase B is dipped to 413V (2% sag) for Lightning search algorithm. UPQC is activated at 0.08s and it injects a voltage of phase A is 320V and phase B is 300V for MPSO, phase A is 231V and phase B is 222V for GWO, phase A is 80V and phase B is 70V for WOA, phase A is 18V and phase B is 9V for HHO and phase A is 3V and phase B is 2V for LSA in all the three phases. Load voltage is not compensated to 415V for using MPSO, GWO, WOA and HHO is shown in Figure 23 (a), Figure 23(b), Figure 23(c) and Figure 23 (d). The Proposed LSA clearly compensates the sag voltage is 415V and the UPQC injected voltage of phase A is 2V and phase B is 2V, which is shown in Figure 23 (e).

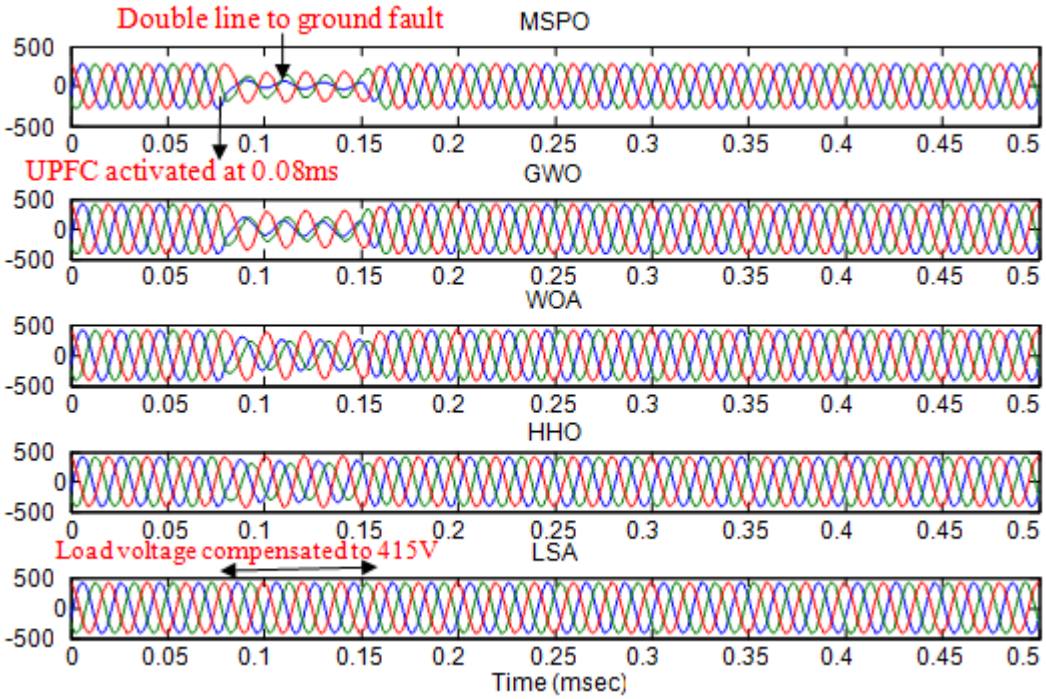

Figure 23: Double Line to Ground Fault Voltage sag Compensation of using MPSO, GWO, WOA, HHO and LSA techniques

A Double line to ground fault occurred at 0.08s and the current in the A phase is dipped to 6A (80% sag) and B phase is dipped to 5A (85% sag) for using Modified particle Swarm Optimization algorithm, A phase is dipped to 12A (50%sag) and B phase is dipped to 14A (45%sag) for using Grey wolf algorithm, A phase is dipped to 16A (40% sag) and B phase is dipped to 17A (30% sag) for using Whale optimization algorithm, A phase is dipped to 20A (13% sag) and B phase is dipped to 21A (10% sag) for Harris Hawks Algorithm and A phase is dipped to 23A (4% sag) and B phase is dipped to 24A (3% sag) for Lightning search algorithm. UPQC is activated at 0.08s and it injects a voltage of A phase is 18A and B phase is 17V for MPSO, A phase is 13A and B phase is 11A for GWO, A phase is 7A and B phase is 9A for WOA, A phase is 5A and B phase is 5A for HHO and A phase is 2A and B phase is 1A for LSA in all the three phases. Load current is not compensated to 25A for using MPSO, GWO, WOA and HHO is shown in Figure 24 (a), Figure 24(b), Figure 24(c) and Figure 24 (d). The Proposed LSA clearly compensates the sag voltage is 25A and the UPQC injected current of A phase is 2A and B phase is 1A, which is shown in Figure 24 (e).

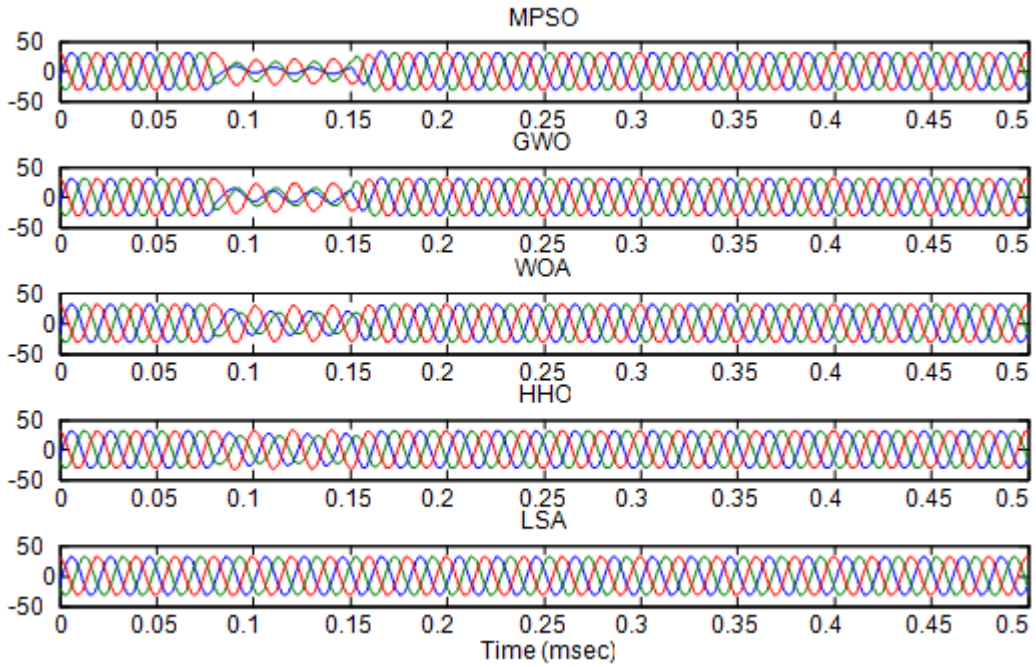

Figure 24: Double Line to Ground Fault current sag Compensation of using MPSO, GWO, WOA, HHO and LSA techniques

Table 1 and Table 2 shows the compensated voltage and current comparison of the proposed and existing techniques. The proposed techniques produce the compensated voltage is low compared to other existing methods are MPSO, GWO, WOA, HHO and LSA.

Table 1: The proposed and existing techniques compensated voltage comparison

Optimization techniques	Three phase fault		Line to line fault				Single line to ground fault		Double Line to ground fault			
	Voltage (V)	Injected Voltage (V)	Phase A	Injected Voltage (V)	Phase B	Injected Voltage (V)	Phase A	Injected Voltage (V)	Phase A	Injected Voltage (V)	Phase B	Injected Voltage (V)
MPSO	190	210	90	320	110	300	120	290	95	320	113	300
GWO	210	192	180	230	190	220	200	195	185	231	190	222
WOA	310	101	320	80	330	70	280	130	315	80	320	70
HHO	390	22	395	18	405	9	395	18	390	18	395	9
LSA	413	2	412	3	413	2	405	10	413	3	413	2

Table 2: The proposed and existing techniques compensated voltage comparison

Optimization techniques	Three phase fault		Line to line fault				Single line to ground fault		Double Line to ground fault			
	Current (A)	Injected Current (A)	Phase A	Injected Current (A)	Phase B	Injected Current (A)	Phase A	Injected Current (A)	Phase A	Injected Current (A)	Phase B	Injected Current (A)
MPSO	5	19	5	18	6	17	7	17	6	18	5	17
GWO	9	13	10	14	12	12	10	14	12	13	14	11
WOA	11	11	16	9	18	7	14	10	16	7	17	9
HHO	18	9	19	5	21	4	19	5	20	5	21	5
LSA	22	3	22	3	24	1	22	3	23	2	24	1

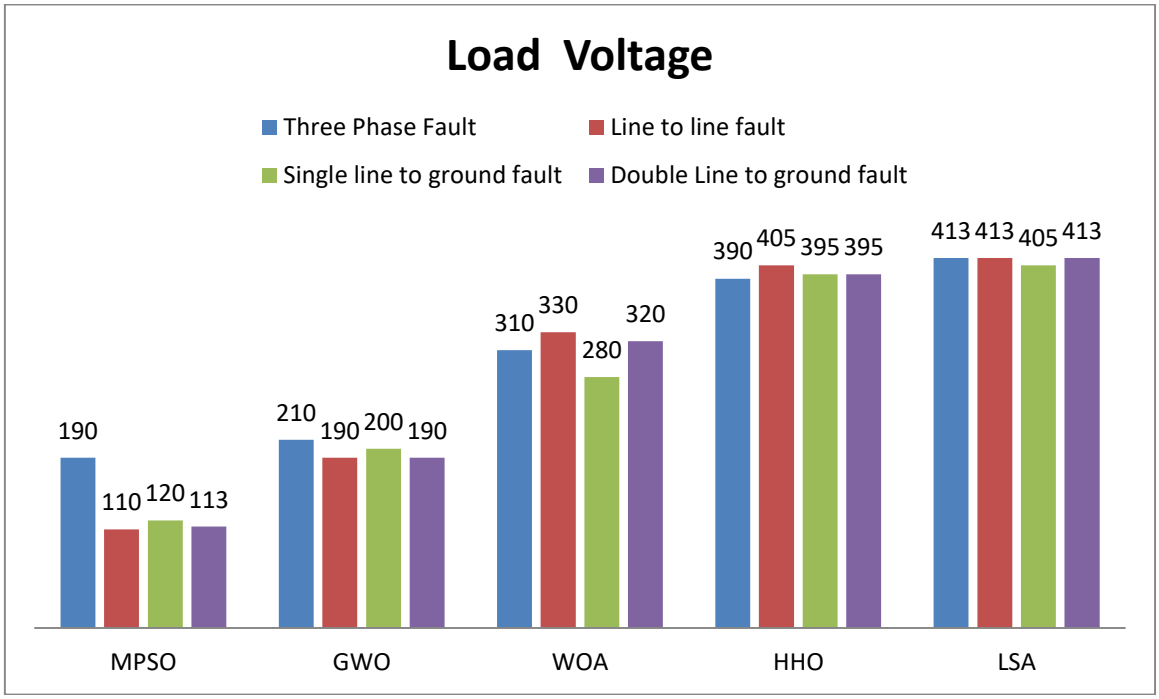

Figure 24: Comparative analysis for sag compensation for various Optimization techniques

Sag compensation comparative analysis is shown in the Figure 24 and from the observed performances is pointed out below.

(i) From the Four control optimization techniques, it is clear that LSA is better than other methods

(ii) The voltage restoration is maximum for using the LSA optimization algorithm.

VI. Conclusion

This paper introduced Lightning Search Algorithm, as a new optimization technique for mitigation of power quality using UPQC controller. The main role of controlled UPQC is to support the voltage compensation for the system during fault events. With the UPQC controlled system, the performance of a grid-connected hybrid system consisting of WECS, PV system and battery can be improved. The controlled UPQC also succeed in increasing the restoration capability of the system and keep the RES connected to the grid during abnormal operating conditions without disconnection. LSA for compensation of voltage sag, current sag for three phase fault condition is introduced in this paper proved better performance when compared to MPSO, GWO, WOA and HHO.

References

[1]. K. S. Latha, M. V. Kumar. Statcom for enhancement of voltage stability of a dfig driven wind turbine. in: 2014 POWER AND ENERGY SYSTEMS: TOWARDS SUSTAINABLE ENERGY, IEEE, 2014, 1–5.

[2]. H. Le-Huy. Performance study of a four-phase 8/6 switched reluctance generator using a nonlinear model based on magnetization curves. in: 2009 35th Annual Conference of IEEE Industrial Electronics, IEEE, 2009, 3910–3915.

[3]. S. Mirjalili, S.M. Mirjalili and A. Lewis, "Wolf Optimizer," Advances in Engineering Software, vol. 69, pp. 46–61, 2014.

[4]. J. Kennedy and R. Eberhart, "Particle swarm optimization." Proceedings of the 1995 IEEE International Conference on Neural Networks, Perth, Australia, vol. 4, pp. 1942–1948, Dec.1995.

[5]. Femia, N., Petrone, G., Spagnuolo, G., & Vitelli, M. (2005). Optimization of perturb and observe maximum power point tracking method. IEEE Transactions on Power Electronics, 20(4), 963–973. https://doi.org/10.1109/TPEL.2005.850975.

[6]. Tafticht, T., Agbossou, K., Cheriti, A., & Doumbia, M. L. (2006). Output power maximization of a permanent magnet synchronous generator based stand-alone wind turbine. Industrial Electronics, 2006 IEEE International Symposium on, 3, 2412–2416. https://doi.org/10.1109/ISIE.2006.295950

[7]. Heidari, A.A.; Mirjalili, S.; Faris, H.; Aljarah, I.; Mafarja, M.; Chen, H. Harris hawks optimization: Algorithm and applications. Futur. Gener. Comput. Syst. 2019, 97, 849–872.

[8]. H.Shareef, AA. Ibrahim, A.H.Mutlag, Lightning search algorithm, Applied Soft Computing, 36, 20I5,pp.3lS-333.

[9]. Thumu, Raghu; Harinadha Reddy, Kadapa; Rami Reddy, Chilakala (2020). Unified power flow controller in grid-connected hybrid renewable energy system for power flow control using an elitist control strategy. Transactions of the Institute of Measurement and Control, (), 014233122095789–. doi:10.1177/0142331220957890.

[10]. A. Ghosh and G. Ledwich, Power Quality Enhancement Using Custom Power Devices, Kluwer Academic Publishers, Boston, Mass, USA, 2002

[11]. Mohammed I. Mosaad, 2020, "Whale Optimization Algorithms-based PI controllers of STATCOM for Renewable Hybrid Power System", World Journal of Modelling and Simulation Vol. 16 (2020) No. 1, pp. 26-40

[12]. Vandana chaudhary,2019," Power quality enhancement using unified power flow controller in grid connected hybrid PV/Wind system", IEEE International Conference on Communication and Electronics Systems, 978-1-7281-1261-9.
[13]. Ghadimi N, Afkousi-Paqaleh A and Emamhosseini A (2013) A PSO based fuzzy long-term multi-objective optimization approach for placement and parameter setting of UPQC. Arabian Journal for Science and Engineering 39(4): 2953–2963.
[14]. Lashkar Ara A, Kazemi A and Nabavi Niaki SA (2011) Modelling of optimal unified power flow controller (OUPQC) for optimal steady-state performance of power systems. Energy Conversion and Management 52(2): 1325–1333.
[15]. Sarker J and Goswami S (2014) Solution of multiple UPQC placement problems using gravitational search algorithm. International Journal of Electrical Power and Energy Systems 55:531–541.
[16]. Dutta S, Roy PK and Nandi D (2015) Optimal location of UPQC controller in transmission network using hybrid chemical reaction optimization algorithm. International Journal of Electrical Power and Energy Systems 64: 194–211.
[17]. E. Babaei et al., 2011, "An improved PSO and genetic algorithm based damping controller used in UPQC for power system oscillations damping", International Conference on Electrical Machines and Systems, DOI: 10.1109/ICEMS.2011.6073818
[18]. Ranjan Kumar Mallick et al., 2016, "Design of GWO optimized dual UPQC controller for damping of power system oscillations", IEEE Uttar Pradesh Section International Conference on Electrical, Computer and Electronics Engineering (UPCON), DOI: 10.1109/UPCON.2016.7894678
[19]. K. Aravindhan et al., 2019, "Optimal Placement and Co-ordination of UPQC with DG Using Whale Optimization Algorithm (WOA)", Emerging Trends in Computing and Expert Technology pp 375-386
[20]. Mohammad Zohrul Islamet al., 2019, "Optimal Power Flow using a Novel Harris Hawk Optimization Algorithm to Minimize Fuel Cost and Power loss", IEEE Int. J. Electr. Eng. Informatics vol. 65, pp. 360–373, 2019
[21]. Serhat Duman,2019, "Solution of the Optimal Power Flow Problem Considering FACTS Devices by Using Lightning Search Algorithm", Iranian Journal of Science and Technology - Transactions of Electrical Engineering 43(3):1-29, DOI: 10.1007/s40998-019-00199-2

Ms Geena.S, et. al. "Lightning Search Algorithm For Mitigation Of Power Quality Using UPQC Controller: A Comparative Approach." *IOSR Journal of Electrical and Electronics Engineering (IOSR-JEEE), 18(3),* 2023, pp. 01-23.